Fatigue Behavior of Concrete in Anchor System

Zaidir *, Kyuichi MARUYAMA **, Takumi SHIMOMURA ***, Tsuyoshi TAKAHASHI ****

* Grad. Student, Dept. of Civil Engg., Nagaoka Univ. of Technology, 1603-1, Kamitomioka-machi, Nagaoka 940-21.
** Ph.D., Professor, Dept. of Civil Engg., Nagaoka Univ. of Techn.,1603-1, Kamitomioka-machi, Nagaoka 940-21.
*** Dr.of Eng., Associate Professor, Departement of Civil Engineering, Nagaoka University of Technology, 1603-1, Kamitomioka-machi, Nagaoka 940-21.
**** M. of Eng., Member of JSCE, Mitsui Construction Co. Ltd.

Fatigue behavior of concrete has received considerable attention in the last two decades. However, the knowledge about the cause and mechanism of concrete fatigue fracture is still limited and not well understood. This paper discusses the fracture process and crack growth in concrete conducting the pull-out test of an anchor bolt under fatigue loading. A simple model of fatigue fracture mechanism is introduced and the fatigue strength of concrete in tension and shear is discussed referring to the formula proposed by the Japan Society of Civil Engineers (JSCE).

Key Words : fatigue behavior, crack growth, fatigue strength, pull out test of anchor bolt

1. Introduction

In the last two decades, the fatigue behavior of concrete has received considerable attention from researchers in the field of concrete structures. There are several reasons for this interest, for instance, it is recognized that even if cyclic loading does not cause a fatigue failure, it may lead to inclined cracking in structural members, or may cause cracking in component materials of member which alters the static load carrying characteristics. Until now, the knowledge about fatigue behavior of concrete, however, is still limited and not well understood, specially in terms of the cause and mechanism of failure and crack growth, because the difficult and tedious experiments are required for conducting research investigations.

In the past, most studies on the fatigue of concrete have so far been directed to interrelated the applied-fatigue stress and the fatigue life of concrete only[1)-6)]. The relationship is shown by so-called *S-N* curves which enables one to predict the mean fatigue life of concrete for each relative stress level. Although these investigations were very valuable from a practical point of view, they do not explain the cause and mechanism of crack growth in concrete fatigue fracture.

Since a remarkable progress has been accomplished in the application of fracture mechanics to concrete with the existence of fracture process zone (FPZ) on static crack growth, it is expect that the knowledge could be extended to fatigue crack growth with proper modification.

This paper discusses the crack growth and fracture process in concrete under fatigue loading by the pull out test of an anchor bolt. First, the static pull-out test is conducted to study the applicability of ink-injection for measuring the crack growth in concrete. Then, the cyclic pull out test is performed and a simple model of fatigue fracture mechanism is introduced. Finally, the fatigue strength of concrete in tension and shear[7)] is discussed in comparison of the experimental data with both the calculation by the model and the formula proposed by Japan Society of Civil Engineers (JSCE).

2. EXPERIMENT

2.1 Specimens

In order to study the fatigue behavior of concrete by an anchor bolt system, the anchor bolt was chosen as to cause concrete cone failure. The type of anchor bolt was headed anchor which was placed in formwork before

Table-1. The properties of bolt and concrete block

Bolt Type	JIS B 1180-1974
1.Max Tensile Strength of Bolt	1059 MPa
2.Diameter of Bolt	16 mm 20 mm
3.Embedment Length	30 mm 45 mm
Dimension of Block	400x400x250mm
1.Compressive Strength	31.9 MPa
2.Splitting Tensile Strength	2.6 MPa

casting concrete. The frictional resistance between a bolt and concrete was eliminated by wrapping the bolt shaft with vinyl tape.

In this experiment two types of diameter of bolt, 16 mm and 20 mm were used with the embedment lengths of 30 mm and 45 mm, respectively.

Fig.-1 shows the concrete block specimen. It has dimension of 400 mm x 400 mm x 250 mm. Four pieces of aluminum sheath with diameter of ϕ 20 mm were embedded at a corner of block which will be used for mounting reaction points of specimen. The used concrete is ready mix concrete with a maximum of aggregate size of 25 mm and design slump value of 100 mm. The compressive and tensile strengths of concrete were obtained using a companion cylinder specimens of ϕ100mmx 200mm which were cured in the same condition until one month old. All properties of bolt and the concrete block were summarized in **Table-1**.

Two series of specimens were prepared in two times of concrete casting referred to series A and series B for static and fatigue test, respectively.

In all fatigue test, the load was applied by a sine wave form and fluctuated between a constant minimum load level, P_{min} = 10% of ultimate capacity, P_u and maximum load level, P_{max} from start until failure or until 2 million load cycles. The values of P_{max} were 60%, 70% and 80% of P_u as shown in **Table-2**. The loading was performed at a frequency of 5 cycles per second (5 Hz).

Prior to the fatigue test, four specimens of series B for each embedment length were tested statically to estimate the static pull-out strength as the basis for determining load levels in the fatigue test.

In order to observe crack growth in concrete, a number of narrow holes for injection of ink were provided around a bolt by placing piano wires before casting concrete. Holes were constructed by pulling out wires after hardening of concrete. The diameter of hole was 1.2 mm and the length was about the same as the embedment length of a bolt. To investigate the influence of holes to load carrying capacity, two types of hole number were used, namely 48 holes and 72 holes, respectively as shown in **Fig.-2**.

Table-2. Load levels of fatigue loading

Embedment length, h_e		30 mm	45 mm
Ultimate load (ave.), P_u		13.73kN	29.81kN
P_{max}/P_u	80%	10.98kN	23.85kN
	70%	9.61kN	20.87kN
	60%	8.24kN	17.89kN
P_{min}/P_u	10%	1.37kN	2.98kN

P_{max}: maximum load level, P_{min} : minimum load level
P_u : static ultimate load (average)

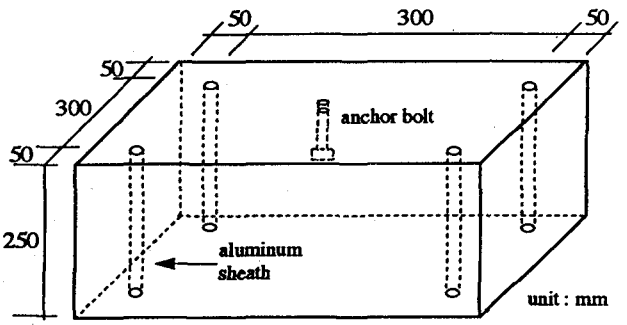

Fig.-1 Concrete block

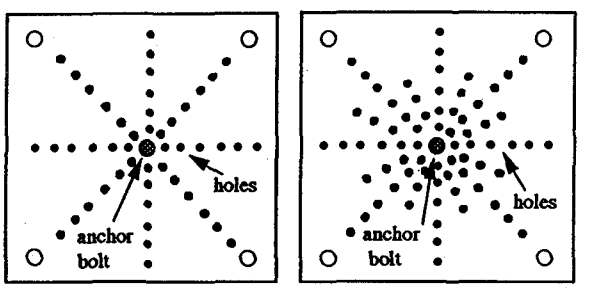

(a) with holes in 8 directions (48 holes)

(b) with holes in 16 directions (72 holes)

Fig.-2 Location of holes around bolt

2.2 Test Procedures

Experiments were conducted using a dynamic servo actuator loading machine which was used in both static and fatigue loadings as shown in **Fig.-3**. The loading machine has a load cell of 49 kN capacity with a reaction frame, a control panel and A/D converter. All measured data were recorded and stored through a personal computer.

A schematic representation of the test is shown in **Fig.-4**. At a certain load level from lower level up to near maximum for static test, or at a certain number of load cycles for fatigue test, the ink-ethanol solution was injected into concrete through holes by a injection. The penetration time of ink was about 20 minutes and after that the remained ink in holes was vacuumed and dried

using a hairdrier for about 5 minutes. The used ink are ordinary ink with a vivid black and blue colors. Its viscosity is 1.41 x 10^{-2} P_o and molecular dimension ranges from10^{-2} μm to 10 μm. After failure occurred, the crack pattern dyed by ink for each specimen was recorded in photograph and with help of a scanner and computer calculation the area of cracked section was obtained.

In order to eliminate the influence of compressive stress produced near the reaction points on the stress transfer mechanism, the distance between reaction points was designed more than six times of the embedment length as shown in **Fig.-4**.

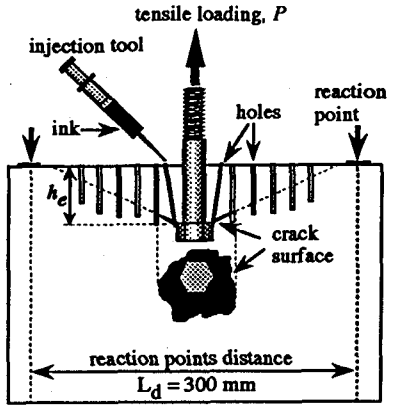

Fig.-4 Testing method

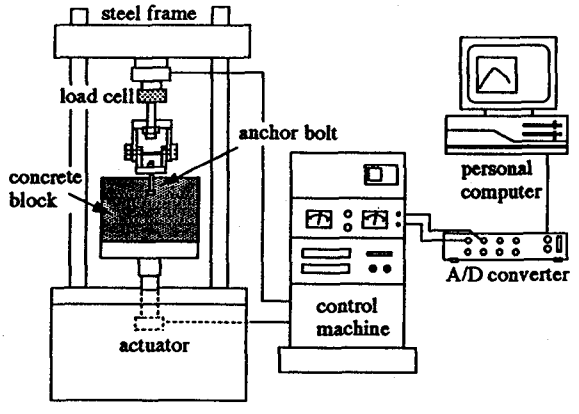

Fig.-3 Testing system

3.TEST RESULTS AND DISCUSSIONS

3.1 Static Test Results

Thirty specimens of series A plus eight specimens of series B for two cases of embedment length were tested in the static condition. All specimens showed the concrete cone failure. **Table-3(a)** and **3(b)** summarize the static test results for both cases of embedment length.

Fig.-5 show the shape of failed concrete cone for both types of embedment length. The inclination angle between a failure cone and the surface of concrete, θ ranged from 15°~40°, with average values of 24° and 28° for embedment lengths of 30 mm and 45 mm, respectively. The average inclination angle, θ tended slightly to increase with increase of embedment length.

Table-3(a) Static test results, for embedment length, h_e= 30 mm

Specimens no.	Number of holes	Inclination angle θ_L(°)	Inclination angle θ_R(°)	P_u (kN)	Load at ink injection, P (kN)	Total area of cone A_{cone} (mm²)	Total area of ink A_{crack} (mm²)	Failure mode
SH30N-1	No holes	30.0	22.6	12.56	–	–	–	Cone failure
SH30N-2		21.8	39.8	15.01	–	–	–	"
SH30N-3		25.5	19.0	14.81	–	–	–	"
SH30-4	8 directions (48 holes)	27.8	23.5	17.66	1.47	58178.9	392.5	Cone failure
SH30-5		22.6	23.5	16.97	1.96	69150.7	506.3	"
SH30-6		17.4	21.0	17.76	2.94	54931.1	557.3	"
SH30-7		32.0	19.7	17.27	2.94	61766.2	551.0	"
SH30-8		35.5	23.5	16.78	5.89	65615.1	1094.5	"
SH30-9		23.5	23.5	17.67	5.89	65322.5	444.2	"
SH30-10		32.0	30.5	17.76	7.36	47659.7	445.5	"
SH30-11		32.0	18.4	16.28	7.36	47185.1	692.6	"
SH30-12		29.1	21.0	17.27	9.81	66469.9	1088.6	"
SH30-13	16 directions (72 holes)	24.4	21.0	18.15	9.81	60901.6	811.5	Cone failure
SH30-14		15.5	15.0	20.11	12.75	66590.2	997.4	"
SH30-15		22.6	24.4	18.84	12.75	56878.0	884.3	"
SH30-16		19.0	19.7	18.64	15.70	67886.4	1199.2	"
SH30-17F		25.2	32.4	14.22	9.81	53012.8	674.2	"
SH30-18F		22.3	30.4	15.21	14.72	69020.4	10787.4	"
SH30-19F		23.6	33.2	11.97	9.81	51602.2	4247.7	"
SH30-20F		25.2	32.4	13.54	9.81	48257.3	765.0	"

Table-3(b) Static test results, for embedment length, h_e= 45 mm

Specimens no.	Number of holes	Inclination angle θ_L(°)	Inclination angle θ_R(°)	P_u (kN)	Load at ink injection, P (kN)	Total area of cone A_{cone} (mm²)	Total area of ink A_{crack} (mm²)	Failure mode
SH45N-1	No holes	34.6	30.5	27.27	--	--	--	Cone failure
SH45N-2		22.6	30.5	29.14	--	--	--	"
SH45-3	8 directions (48 holes)	22.6	25.5	33.06	4.91	100351.3	316.0	Cone failure
SH45-4		45.0	35.5	35.61	2.94	96805.0	411.0	"
SH45-5		19.3	35.5	38.46	1.96	80210.8	431.6	"
SH45-6	16 directions (72 holes)	33.7	29.7	31.88	24.53	75493.6	1957.8	Cone failure
SH45-7		26.6	17.9	36.20	29.43	121726.7	3915.6	"
SH45-8		18.7	24.0	37.28	31.88	111406.8	3438.5	"
SH45-9		21.0	36.5	32.37	29.43	92374.2	6007.4	"
SH45-10		30.5	30.5	34.92	32.37	111769.5	6183.2	"
SH45-11		19.0	24.0	32.96	19.62	110928.4	1709.4	"
SH45-12		27.8	23.5	32.86	14.72	109960.5	838.9	"
SH45-13		28.4	15.1	32.67	9.81	105135.2	774.9	"
SH45-14		25.5	20.3	38.55	6.87	121314.8	1093.5	"
SH45-15F		32.7	32.2	28.15	19.62	104286.7	2588.7	"
SH45-16F		23.6	42.6	37.38	24.53	96363.4	3285.9	"
SH45-17F		22.6	34.4	29.63	9.81	117647.6	1585.3	"
SH45-18F		33.3	32.2	24.23	--	--	--	"

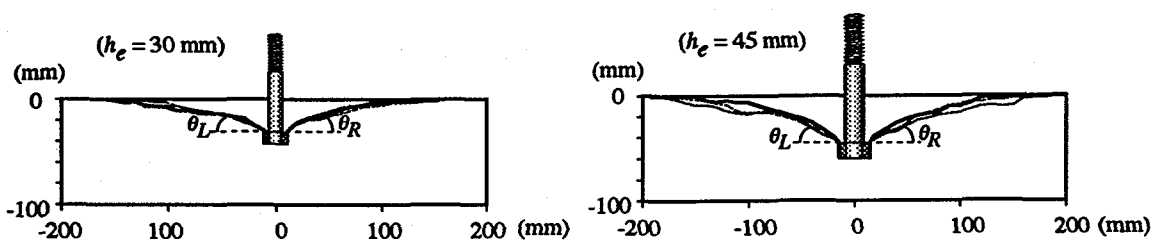

Fig.-5 The shape of failed concrete cone

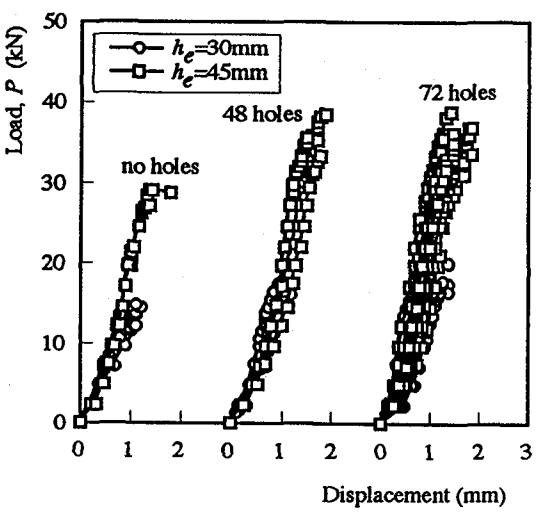

Fig.-6 Load-displacement curves with and without holes

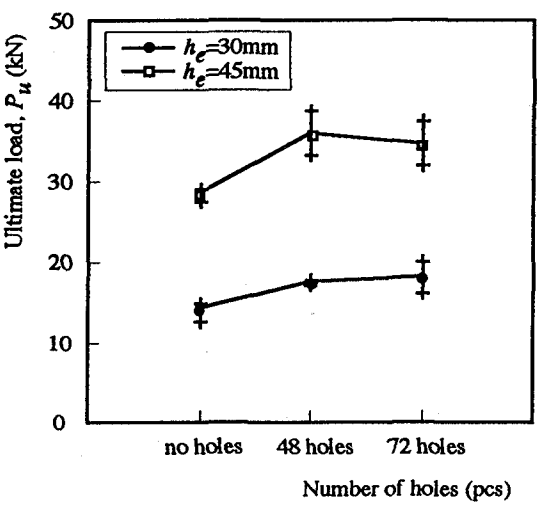

Fig.-7 Influence of hole number on ultimate capacity

Load -displacement curves with and without holes are shown in **Fig-6. Fig.-7** shows the influence of the number of holes on the ultimate capacity. From these figures, it can be seen that no significant effect of holes is observed on the load carrying capacity of anchor bolts with concrete cone failure.

A process of crack growth with increase of load is shown in **Fig.-8** for both cases of embedment length. No significant difference in crack growth could be recognized. The ratio of crack cone surface area to total cone surface area is plotted as a function of the ratio of applied load to the ultimate capacity. The results are

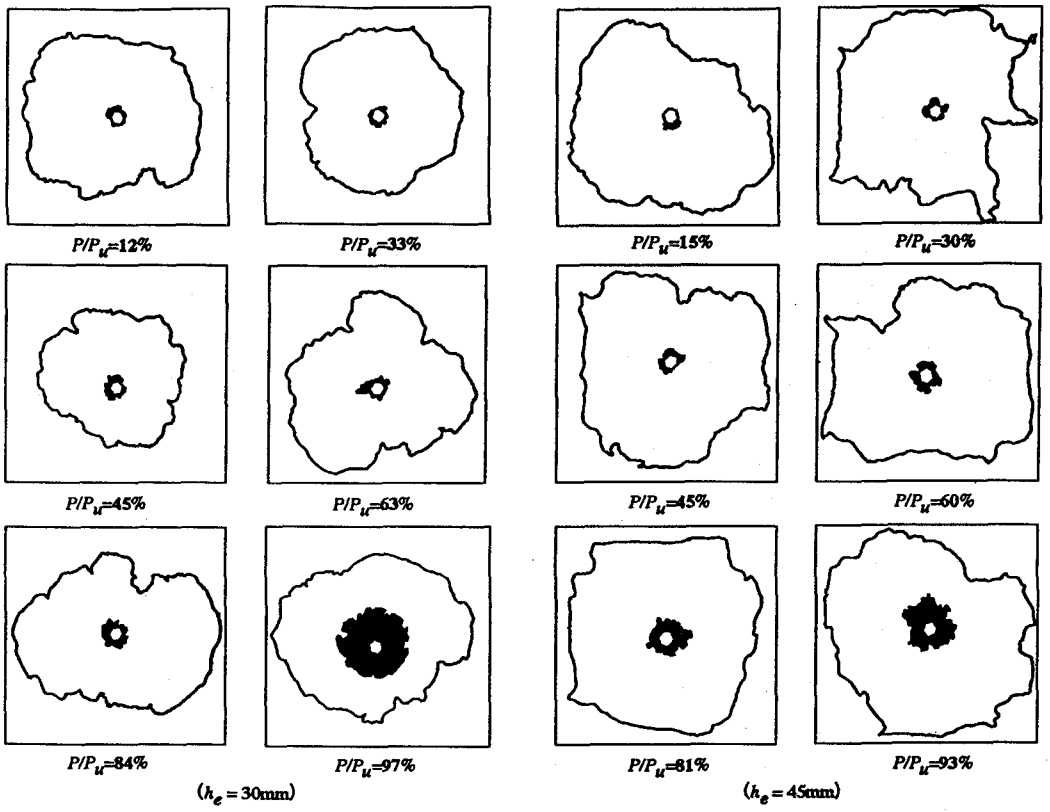

Fig.-8 Process of crack growth with increase of applied load

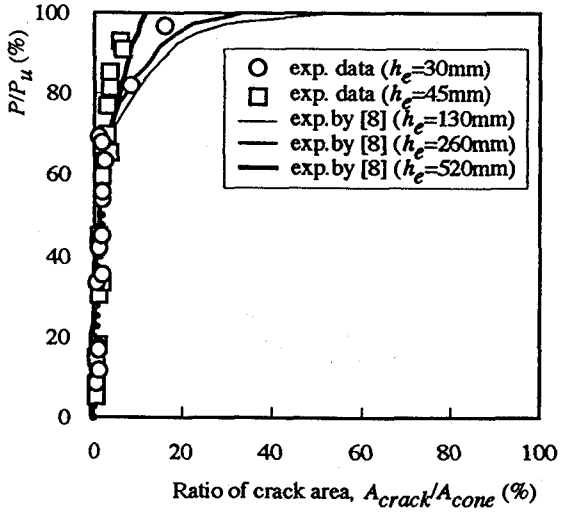

Fig.-9 Ratio of crack surface area as function of load with comparison to exp. by [8]

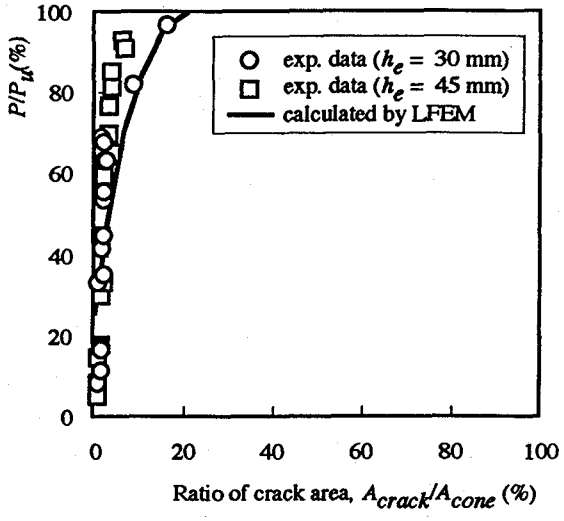

Fig.-10 Ratio of crack surface area as a function of load with comparison to LFEM calculation

shown in **Fig.-9** in comparison with the results of Eligehausen &Sawade[8]. **Fig.-10** shows the comparison of test results with a calculation of Linear Finite Element Analysis. From these figures a crack growth mechanism could be summarized as the following steps:

(1) Circumferential crack in concrete starts at an early loading level, about 10% of the maximum capacity near the edge of the head of bolt. The distribution of crack in concrete is not necessarily symmetric about the axis of bolt, but the crack initiates at someplace with lowest stress near the head of bolt. Experimental observation showed that the cracks normally started at the mortar matrix of concrete.

(2) Cracks continue to grow with increase of applied load, but until about 90% of the ultimate capacity is reached, the cracks grow slowly near the edge of a bolt.

(3) Near the ultimate capacity unstable cracks grow fast and a concrete cone failure is fully developed.

Based on the results it could be concluded that the applicability of ink injection technique to trace crack growth in concrete proved effective.

3.2 MODELING OF FATIGUE FAILURE MECHANISM.

In this paper an attempt is made to explain the fatigue behavior of concrete based on the crack growth under fatigue loading. In the fracture mechanics of concrete, Hillerborg and co-workers[13] proposed the fictitious crack (also called fracture process zone, FPZ) ahead of a visible crack. In the fictitious crack zone (FPZ), stresses can still be transferred, depending on the crack opening displacement as shown in **Fig.-11**. Up to date, the length of the fracture process zone obtained by testing and computing are distinct from each other[16),17)].

For static loading of anchor bolt, Maruyama. K et.al[1)] and Eligehausen & Sawade[8)] reported that the maximum load was reached when a relative crack length a/L went up to 0.45. Taking these results into account, the stress resistant mechanism under fatigue loading was modeled on the following assumptions:

(1) Circumferential crack begins to propagate when the stress at a crack tip exceeds the ultimate tensile strength of concrete, f_t given by the standard test.

(2) After the first cycle of loading there is an initial crack at the edge of a bolt with a length depending on the level of fatigue loading. This crack propagates due to a number of cycles of loading at an angle of θ as shown in **Fig.-12**. (θ is an average value obtained from the experiment results, 27 degree in this case)

(3). At the tip of crack there act tensile and bending stresses. The applied load is resisted by both the elastic strength of the uncracked portion of concrete and the bridging or interlocking action of the cracked portion. The distribution of resistant stress is assumed to be a triangle shape as shown in **Fig.-13**.

The crack forms a cone and that the crack tip must penetrate through a larger area as the crack gets longer. This implies that for a constant amplitude of cyclic loading the tensile stress at the crack tip decreases as the crack length increases. However, the bending stress at the crack tip increases because the diameter of conical shape of cracked portion increases and the cross sectional area decreases by propagation of crack.

The tensile stresses, σ_{tn} at the crack tip at any crack length, a_n is given as,

$$\sigma_{tn} = \frac{P}{\pi (a_f + b) X_n} \cos\theta^{-1} \qquad (1)$$

where, a_f and b denote the stress acting lengths at cracked (FPZ) and uncracked zone at the N^{th} cycle of loading. The length of a_f equal to crack length, a_n when $a_n < 0.45\ a/L$. The length of b is assumed to be constant along propagation of crack. X_n is the distance of resultant of force of stress distribution to the center of a bolt.

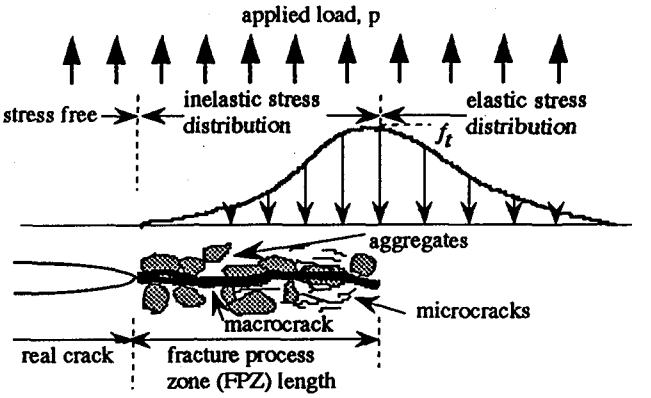

Fig.-11 Schematic of fracture process zone (FPZ) concept in concrete

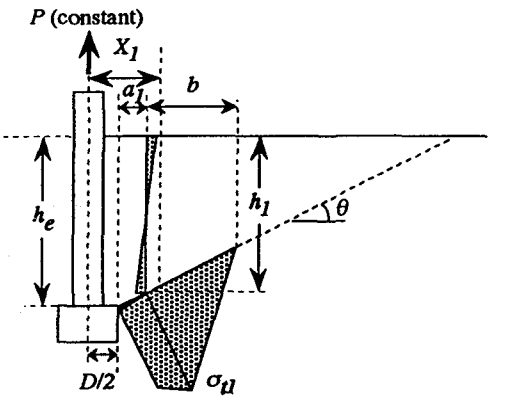

Fig.-12 Model of stress-resistant mechanism after 1^{st} cycle

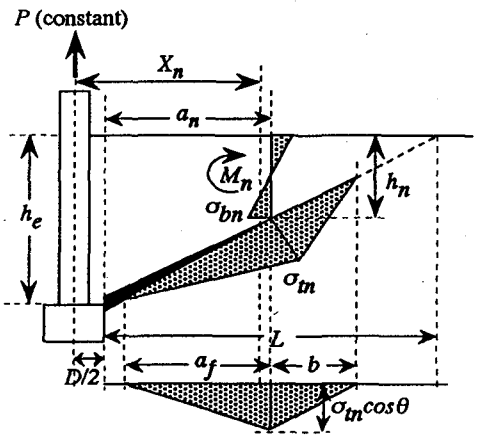

Fig.-13 Model of stress-resistant mechanism after N^{th} cycle

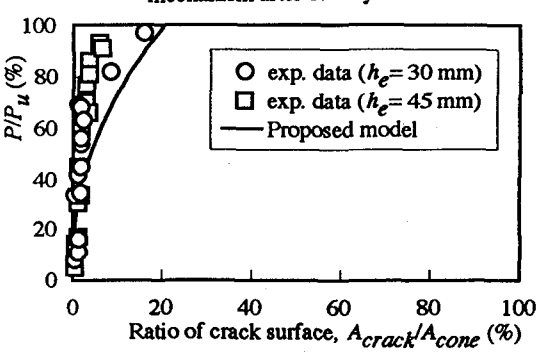

Fig.-14 Calculated crack growth and test results of static loading

P denotes the applied cyclic load.

The bending moment, M_n and bending stress, σ_{bn} at any crack length are given as,

$$M_n = 0.125\left(2a_n + D\right)P \qquad (2)$$

$$\sigma_{bn} = \frac{0.375\,P}{\left(a_n + D/2\right)\pi^2 h_n^2} \qquad (3)$$

$$h_n = h_e - a_n \sin\theta$$

where, h_n denotes a distance between a tip of crack to surface of concrete and h_e is an embedment length. D denotes the diameter of bolt head.

The total stress at crack tip, σ_{sn} at any crack length is given as,

$$\sigma_{sn} = \sigma_{tn} + \sigma_{bn} \qquad (4)$$

From **Eq.(1)**, when a crack gets longer under a constant cyclic load P, the tensile stress decrease, but on the other hand the bending stress from **Eqs.(2)** and **(3)**, increase as the crack length increases.

Fig.-14 shows the calculated crack growth by the model in comparison to with the test results under static loading. The model has a good agreement with the test results.

Fig.-15 shows the variation of tensile, bending and total stresses at the crack tip as a function of crack length for the load levels of 60%, 70% and 80%. From this figure, it could be seen that in the beginning the total stress decreases with increase of crack length, but at a certain point the total stress turns to large with increase of bending stress, and increases until failure occurs.

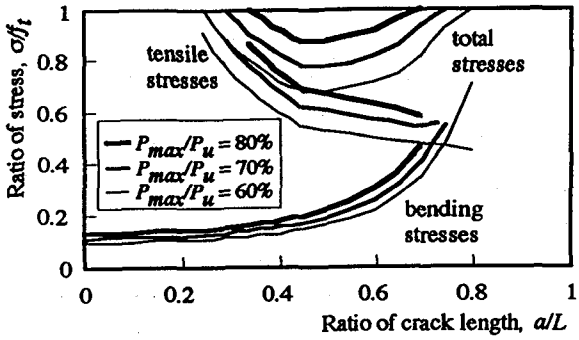

Fig.-15 Variation of stress at crack tip as a function of crack length

3.3 FATIGUE STRENGTH OF CONCRETE

Japan Society of Civil Engineers (JSCE)[18] has proposed an equation to predict the fatigue strength of concrete in compression, flexural compression, tension and flexural tension as follow,

$$log\ N = 17\left(1 - \frac{\sigma_{max} - \sigma_{min}}{f_u - \sigma_{min}}\right) \qquad (5)$$

Table.-4(a) Fatigue test results, for embedment length, h_e = 30 mm

Specimens no.	Load level P_{max}/P_u (%)	Inclination angle θ_L (o)	Inclination angle θ_R (o)	Cycles at failure N_f (cycles)	Cycles at ink injection, N (cycles)	Total area of cone A_{cone} (mm^2)	Total area of ink A_{crack} (mm^2)	Failure mode
F8H30-1	80	30	47.7	3740	100 1000	1602.620 2241.958	35020.492	Cone failure
F8H30-2		28.9	25.2	1515	100 1500	2667.348 9192.607	33353.075	"
F8H30-3		24.1	33.9	3780	500 2000	2750.985 3466.756	41884.998	"
F8H30-4		33.1	22.5	4465	500 4200	4695.300 12116.800	55349.300	"
F8H30-5		25.1	37.2	7380	2000 7300	4191.000 8913.200	43332.200	"
F8H30-6		30.5	27.2	3375	3000	10963.700	42745.000	"
F7H30-1	70	26.0	39.2	1825	100 1000	2411.738 4681.843	47786.582	"
F7H30-2		26.0	26.6	24815	100 5000	540.084 1379.901	40049.054	"
F7H30-3		25.4	25.4	39635	400 15000	1144.965 3982.048	51901.088	"
F7H30-4		28.6	27.0	348150	10000 335000	765.000 7335.700	51753.900	"
F7H30-5		17.4	27.8	114435	10000 100000	2510.100 8013.200	47766.800	"
F6H30-1	60	21	19.7	1112340	100 500000	824.200 4413.703	78475.754	"
F6H30-2		---	---	2000000	---	---	---	Not failured
F6H30-3		---	---	2000000	---	---	---	Not failured

Table.-4(b) Fatigue test results, for embedment length, h_e= 45 mm

Specimens no.	Load level P_{max}/P_u (%)	Inclination angle θ_L (^{o})	Inclination angle θ_R (^{o})	Cycles at Failure N_f (cycles)	Cycles at ink injection, N (cycles)	Total area of cone A_{cone} (mm^2)	Total area of ink A_{crack} (mm^2)	Failure mode
F8H45-1	80	---	---	4760	---	---	---	Cone failure with splitting
F8H45-2		---	---	31	---	---	---	Cone failure
F8H45-3		35.5	47.7	4990	100 1000	3892.387 7241.943	129357.104	"
F8H45-4		29.7	25.2	1295	100 1000	9528.023 14646.175	113284.687	"
F8H45-5		33.1	33.9	16835	300 1500	2427.642 4306.814	107702.929	"
F8H45-6		31.0	22.5	3380	1000 3000	5455.200 10860.300	87733.000	"
F7H45-1	70	36.4	37.2	6760	100 1000	1357.902 4510.738	116782.095	"
F7H45-2		39.8	27.2	7395	100 5000	2674.794 12250.771	117284.858	"
F7H45-3		29.1	46.8	22120	1000 5000	904.006 3830.677	97503.277	"
F7H45-4		15.9	25.1	42945	10000 42900	6867.000 30379.7	101724.900	"
F6H45-1	60	33.3	32.2	584140	1000 10000	368.979 6038.133	104464.889	"
F6H45-2		---	---	2000000	---	---	---	Not failured
F6H45-3		29.7	27.2	160750	50000 100000	6650.532 8308.200	109100.953	Cone failure
F6H45-4		---	---	2000000	---	---	---	Not failured

where σ_{max} , σ_{min} denote the maximum and minimum stresses and f_u denotes the static strength.

Assuming the stress acting area is constant, **Eq.(5)** could be rewritten in terms of applied forces as,

$$log\ N = 17\left(1 - \frac{P_{max} - P_{min}}{P_u - P_{min}}\right) \qquad (6)$$

where P_{max} , P_{min} denote the maximum and minimum applied loads and P_u denotes the static ultimate capacity.

Experimental data of fatigue test are summarized in **Table-4(a)** and **4(b)**. Twenty-eight specimens were tested in this experiment. Four specimens of 60% load level did not fail until 2 million cycles of load. These specimens then were loaded statically until failure. All failed specimens showed the concrete cone failure. The typical displacement as a function of cycles of load is shown in **Fig.-16**. **Fig.-17** shows the ratio between crack surface area and total cone surface area which is plotted as a function of the ratio of load cycles to the cycles at failure, N/N_f for two cases of embedment length with three load levels. No significant difference in crack growth could be recognized. From these figures, as in the static test results, the propagation of circumferential crack in fatigue test grows slowly until about 90% of failure cycles. Cracks increase significantly near failure. This also was assured by rapid increase of displacement as shown in **Fig.-16**.

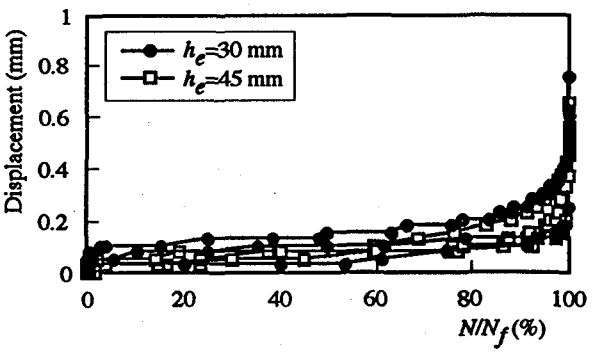

Fig.-16 Typical displacement curves with life ratio, N/N_f

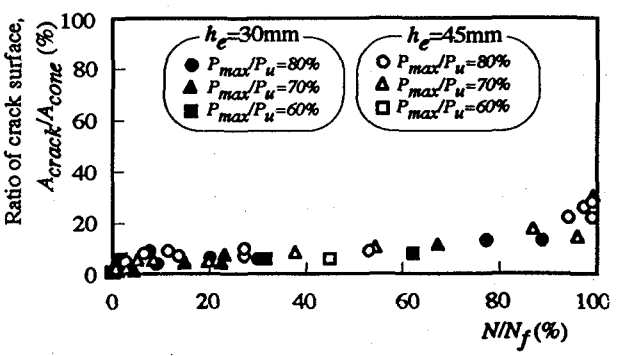

Fig.-17 Ratio of crack surface area with life ratio, N/N_f

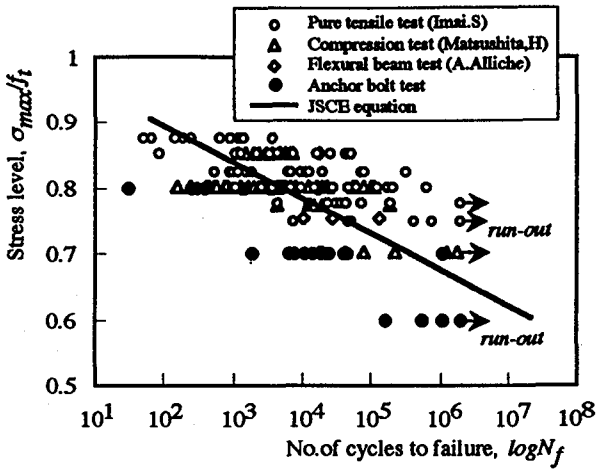

Fig.-18 Fatigue strength of concrete cone failure and comparison to other results

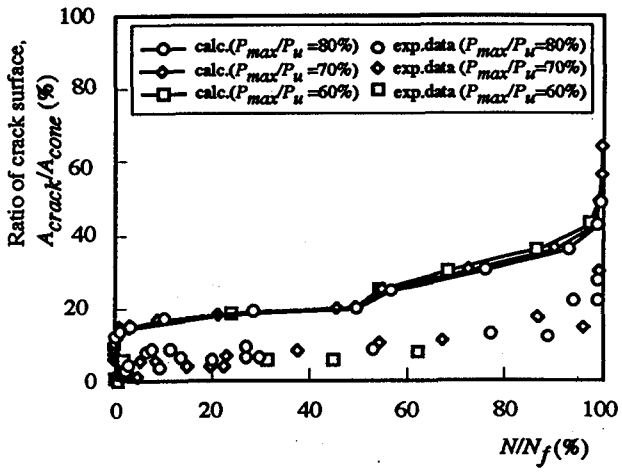

Fig.-20 Ratio of crack surface area with life ratio

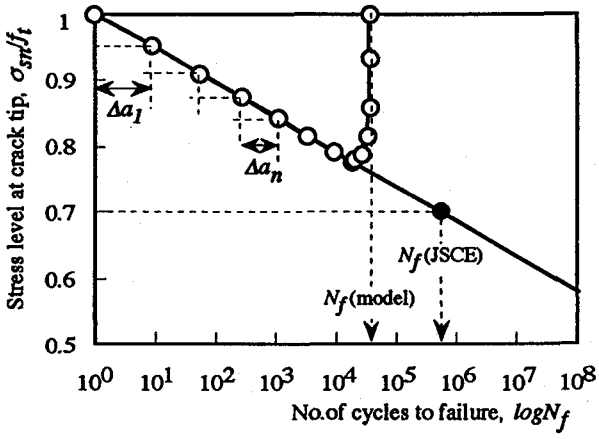

Fig.-19 Calculation of fatigue strength of concrete cone failure by proposed model

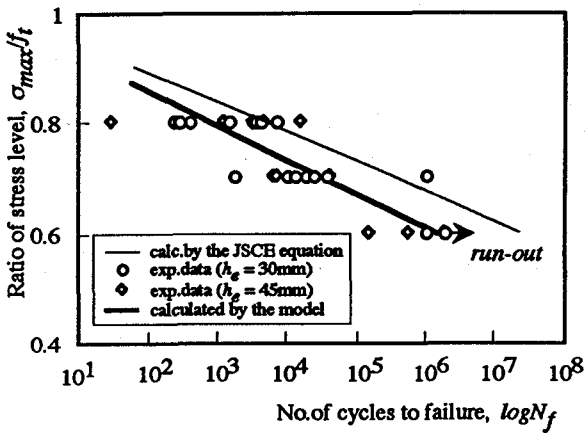

Fig.-21 Fatigue strength of concrete cone failure in comparison to the model and JSCE equation

Fig.-18 shows the experiment results and calculated ones of fatigue strength by **Eq.(5)** in comparison with others. Taking account of scattering of fatigue test data it can be seen that the fatigue strength of concrete under pure tension or flexure could be predicted well by **Eq.(5)**, but that for the cases of concrete cone failure under a combination of tensile and shear stresses the equation looks somewhat unsafe. It might be attributed to the fact that the **Eq.(5)** was originally based on the experimental results of the fatigue strength of concrete under uniaxial compression with a constant stress. As far as the nature of fatigue strength is concerned, **Eq. (5)** could be used to predict the fatigue strength of concrete cone failure under combination tensile and shear stresses. By using a variation of total stress model as shown in **Fig.-15** as a function of crack length, the **Eq. (5)** is again applied to calculate the fatigue strength of concrete in an anchor bolt system.

Fig.-19 shows how to calculate the fatigue strength of concrete using the variation of total stress and an equation of JSCE. After the first cycle there is an initial crack a_1 with a total stress level, σ/f_t at the crack tip equal to unity. After a number of cycles of load, crack propagates with a certain length and the total stress decreases to a certain level as shown in **Fig.-15**. A number of cycles of load that is required to create a certain crack length is calculated by an **Eq.(5)**. This procedure is again applied for the new stress level and crack length until failure occurs. The fatigue strength is cumulative number of cycles of load that is required to create the total crack length to failure.

Fig.-20 shows the calculated crack growth by a proposed model comparing to the test results as a function of cycles of load. In general the proposed model could represent the tendency of crack growth.

Fig.-21 shows the fatigue strength of the test and the calculated results by the proposed model as well as that by an equation of JSCE. Judging from this figure, the calculated result by the proposed model shows a good agreement with the test results.

4. CONCLUSIONS

From this study the followings could be concluded :

1. Until about 90% of the ultimate capacity under static loading the circumferential crack of concrete cone grows slowly and concentrates near the edge of bolt.
2. A testing method of injection of ink-ethanol solution could be proved effective to trace crack growth in concrete.
3. During fatigue loading, the displacement and crack growth increase approximately linearly with the function of cycles of load until 90% of cycles of failure. Just prior to the fatigue failure, the displacement and crack growth increase significantly.
4. Fatigue strength of concrete under pure tension or flexural tensile stress could be predicted well by proposed equation of JSCE, but for the cases of concrete cone failure under combination of shear and tensile stresses the equation looks somewhat unsafe.
5. A model of crack growth mechanism for concrete cone failure under tension and shear was introduced. The model can express the fatigue strength of concrete fairly well.

ACKNOWLEDGEMENT

The authors acknowledge the financial support for this study given by a Grant-in-Aid from the Ministry of Education.

REFERENCES

1) Maruyama, K.,Momose, M.and Shimizu, K., Mechanical Behavior of Undercut Type Fixings, *Transactions of the JCI*, Vol.11,pp.531-538, 1989.

2) Elfgren,L.,et.al., Fatigue of Anchor Bolts in Reinforcement Concrete Foundations, *IABSE Colloquium*, Lausanne,pp.463-470, March 1982.

3) Saito, M. and Imai, S., Direct Tensile Fatigue of Concrete by Use of Friction Grips, *Journal of ACI*, Vol.80, No.9, pp.431-438, 1983.

4) Tepfers, R., Tensile Fatigue Strength of Plain Concrete, *Journal of ACI*, Vo.76, No.8, pp.919-933, August 1979.

5) Matsushita, H., A Study on Compressive Fatigue Strength of Concrete Both in the Air and in the Water Considered Survival Probability, *Concrete Library of JSCE*,No.2, pp.99-127, Dec.1983.

6) Alliche, A. and Francois, D., Damage of Concrete in Fatigue, *J.of Eng. Mechanics*, Vol.118,No.11,pp.2176-2190,Nov.1990.

7) Malhotra, V. Mohan, In Place Evaluation of Concrete, *Proceedings*, ASCE, V.101, CO2, pp.345-357, June 1975.

8) Eligehausen, R.and Sawade, G., A Fracture Mechanics Based Description of the Pull-out Behaviour of Headed Studs Embedded in Concrete, *in Fracture Mechanics of Concrete Structures (From theory to applications)* edited by L.Elfgren, Chapman and Hall Ltd, London,pp.281-298,1989.

9) Stone, W.C and Carino, N.J., Deformation and Failure in Large-Scale Pullout Test, *Journal of ACI*, pp.501-513, Nov-Dec 1983.

10) Krenchel, H. and Shah,S., Fracture Analysis of the Pull-out Tests, *J.of Material Structures*, Vol. 108, pp.439-445, 1985.

11) Rokugo, K., et.al., Pull-out Test of Anchor Bolts and Examination of Failure Processing by Means of Acoustic Emission, *Proceedings of JSCE 43rd annual meeting*, Part 5, pp.418-419, 1988. (in Japanese)

12) CEB comite euro-internatinal du beton., Fastening to Reinforced Concrete and Masonry Structures, State-or-art report, Part II, *Bulletin D'Information No.206*,pp.283-492, August 1991.

13) Hillerborg, A., Modeer, M. and Petersson P-E., Analysis of Crack Formation and Crack Growth in Concrete by means of Fracture Mechanics and Finite Elements, *Cement and Concrete Research*, Vol.6,pp.773-782,1976.

14). Zaidir, Maruyama, K., Shimomura, T. and Takahashi, T., A Testing Method of Crack Growth in Concrete by Pull-out Test of Anchor Bolt, *Proceeding of JCI*, Vol.18, No.2,pp.575-580, 1996.

15) Takahashi, T., Maruyama, K., Shimomura, T. and Zaidir, Fracture Process of Concrete under Tensile Loading with Use of Anchor Bolt, *Proceeding of JCI*, Vol.18, No.2,pp.587-592, 1996. (in Japanese)

16) Bazant, Z.P., Mechanics of Fracture and Progressive Cracking in Concrete Structures, *In Fracture Mechanics of Concrete : Structural Application and Numerical Calculation*, edited by George C.Sih, A.DiTommaso, Martinus Nijhoff Publishers, pp. 1-85, 1985.

17) Hillerborg, A., Numerical Methods to Simulate Softening and Fracture of Concrete, *In Fracture Mechanics of Concrete : Structural Application and Numerical Calculation*, edited by George C.Sih, A.DiTommaso, Martinus Nijhoff Publishers, pp. 141-170, 1985

18) Japan Society of Civil Engineers., Standard Specification for Design and Construction of Concrete Structures , Part I (Design), p.244, 1986.

19) Hordijk, D.A. and Reinhardt, H.W., Numerical and Experimental Investigation into the Fatigue Behavior of Plain Concrete, *J.of Exp. Mechanics*,pp.278-285, Dec. 1993.

20) Horii, H., Shin, H.C. and Pallewatta, T.M., An Analytical Model of Fatigue Crack Growth in Concrete, *Proc.of JCI*, Vo.12, No.2, pp.841-846, 1990.

(Received September 6, 1996)